

AN ANALYSIS OF THE FIBER-FIBER INTERACTIONS USING THE FRAGMENTATION TEST AND OPTICAL COHERENCE TOMOGRAPHY

*Walter G. McDonough, Gale A. Holmes and Joy P. Dunkers,
National Institute of Standards and Technology, 100 Bureau Drive, Stop 8543
Gaithersburg, MD 20899*

Abstract

Multi-fiber model composites are being used in studies into the nucleation of failure in composites. Results have revealed that the nucleation of critical flaws in unidirectional fibrous composites may rely on the time-dependent redistribution of stress by the viscoelastic matrix. Although their role in flaw nucleation is not clearly understood, shear deformation bands have been detected between fiber breaks. Furthermore, interfacial phenomena have been detected in the matrix by Optical Coherence Tomography.

Background

With the increasing use of advanced composites in structural applications, understanding how to predict and manage failure in composite structures has become critical. To this end, generating relevant materials property data that can be used in a computational program by design engineers to predict composite performance is imperative. In response to this need, test methodologies and a tow-based modeling program are being developed to facilitate the integration of critical materials data into composite analyses. The ultimate goal is to predict reliably composite performance properties, and to do this, micro-mechanics properties that account for the composite environment must be included. To obtain the necessary micro-mechanics parameters, the microstructure of the composite lamina is being characterized and used to guide the selection of appropriate micro-mechanics experiments and analysis techniques. Initially, we are examining the interaction between fibers during fiber fracture, the constituent deformation behavior in the composite environment, and the localized failure behavior of the fiber, matrix and interphase region by using 2-dimensional (2-D) multi-fiber arrays and testing these using the fragmentation test. In addition to visual analysis, we are also using Optical Coherence Tomography (OCT) to image the failure process at the fiber/matrix interface.

In the single fiber fragmentation test (SFFT), a dogbone specimen is made with a resin having a single fiber embedded down the central axis. The sample is pulled in tension and stress is transmitted into the fiber through the fiber-matrix interface. Eventually the fiber breaks at its weakest flaw as the strain is increased. The

fragmentation process can continue upon further loading because of the interaction between the fiber and matrix at the interface. This process of fiber breakage continues until the remaining fiber fragments are all less than a critical transfer length (l_c). At this point, the fragmentation process has reached saturation. Once saturation has been reached, the specimen is allowed to relax back to the unstressed state, the fragment lengths are measured, and then a micro-mechanics model is used to estimate the interfacial shear strength.

Typically, the Kelly-Tyson Model [1], where the matrix is assumed to be elastic-perfectly plastic, is used to calculate the interface strength. Another method that has been used is the Cox Model [2], wherein the matrix is assumed to be linear elastic.

Fragmentation of E-glass fibers during interfacial adhesion tests of an epoxy SFFT specimen have been shown by Holmes et al. [3] to occur when the matrix is exhibiting nonlinear viscoelastic behavior. In addition, previous work in this laboratory has shown that polyisocyanurate SFFT specimens also exhibited nonlinear viscoelastic behavior during fiber fragmentation [4]. Hence, a nonlinear analytical procedure was deemed necessary to more accurately assess the interfacial shear strength at the fiber matrix interface. This analytical procedure is based on the non-linear viscoelastic model developed by Holmes et al. to account for the time dependent and non-linear viscoelastic effects of the matrix during the single fiber fragmentation test. This accounting was done by replacing the Young's modulus used in the Cox equation with the time and strain rate dependent secant modulus. For work in this paper, we extend the above technique to examine 2-D arrays of fibers embedded in a matrix. A critical part of this work is the need to acquire image data on the multi-fiber samples at different images planes throughout the sample. Conventional microscopy used for single fiber micro-mechanics testing has neither the thickness resolution nor the sensitivity to fulfill the requirements for the multi-planar, multi-fiber samples. For these samples, we will use OCT.

OCT uses light in a manner analogous to the way ultrasound imaging uses sound, providing significantly higher spatial resolution (10 to 20) μm albeit with shallower penetration depth. OCT is based upon low-coherence optical ranging techniques where the optical

distance to individual sites within the sample is determined by the difference in time, relative to a reference light beam, for an incident light beam to penetrate and backscatter within the sample. This temporal delay is probed using a fiber optic interferometer and a broadband laser light source. The fiber optic interferometer consists of a single-mode optical fiber coupled with a 50/50 fiber optic splitter that illuminates both the sample and a linearly translating reference mirror. Light reflected from the reference mirror recombines with light back-scattered and reflected from the sample at the 50/50 splitter to create a temporal interference pattern which is measured with a photodiode detector. The resulting interference patterns are present only when the optical path difference of the reference arm matches that of the sample arm to within the coherence length of the source. The incident light beam is scanned and repeated measurements are performed at different transverse positions to generate a two dimensional array which represents the backscattering or back reflection of a cross-sectional plane of the material. This data can be displayed as a gray scale or false color image.

In previous work, OCT has been used to successfully image full-scale epoxy/unidirectional E-glass composites (Figure 1). For this work, we used the OCT to image the damage region around the fibers during and after testing.

Experimental

The initial 2-D multi-fiber arrays have consisted of embedded E-glass fibers coated with 11-aminoundecyl trichlorosilane (11-AUTCS) deposited using self-assembled monolayer (SAM) technology. The SAM technology is being used in a companion micro-mechanics program to probe the effect of covalent bonding, mechanical interlocking, and physico-chemical interactions on the transfer of shear stresses at the fiber-matrix interface.

An apparatus designed to prepare 2-D and 3-D multi-fiber model composites has been constructed. Although the inter-fiber spacing between fibers was comparable to published data on 2-D multi-fiber arrays, modifications to the original design were made to minimize the variability in the spaces between the fibers. These modifications will facilitate the construction of uniform 3-D multi-fiber model composites.

Some of the fragmentation tests were carried out on a hand operated testing apparatus similar to the one described by Drzal and Herrera-Franco [5], with the details of the experiments found in Holmes et al. [6]. During the test, a small step strain was applied manually by turning a knob attached to the movable grip of the apparatus. The strain increments are of the order of 0.1 % strain. After the strain increment, there was a delay of 10 min before the

next step-strain. We determined that the fragmentation process depends on the viscoelastic properties of the matrix, and that 10 min allows sufficient time for nearly all of the fragmentation events at each strain increment to take place. After each test was completed, the specimens were unloaded slowly and allowed to relax to an equilibrium length under zero stress, usually over the course of several hours, and the fragment lengths were again measured. Images of the failure process were taken during and after testing.

We also used an automated fragmentation testing machine that has been described previously [7]. A computer program was written to give the operator maximum flexibility in designing a testing protocol. For the work presented in this paper, we used the same routine that was used in the manual single fiber fragmentation machine.

In this work, the OCT image resolution is 11 μm along the x axis (transverse), 15 μm along the z axis (depth), and 11 μm along the y axis (longitudinal). The average fiber diameter is 15 μm . In order to compensate for the spatial resolution, the images were oversampled at 2 μm in the x and y directions, 3 μm in the z direction.

Results and Discussion

In Figures 2 and 3, fiber fractures with debonding and associated matrix crack formation are shown for a 2-D multi-fiber array composed of E-glass fibers embedded in diglycidyl ether of bisphenol-A epoxy resin cured with meta-phenylene diamine. Although the interfiber spacing, ϕ , is less than four fiber diameters in the array, the fiber breaks in adjacent fibers are not aligned vertically as predicted by theory. The standard uncertainty associated with ϕ is 0.05 fiber diameters. Computational predictions [8] indicate that the stress overload in adjacent fibers is smaller for non-aligned breaks. Hence, the composite toughness is predicted to be higher. The persistent bands between fiber breaks in adjacent fibers is permanent deformation. Although the origin of these deformation regions are not clearly understood, 45° deformation bands emanating from the matrix cracks during the test under tensile conditions have been observed (Figure 4).

Using the same constituent composition, fiber fracture in a multi-fiber specimen with the fibers touching is shown in Figure 5. In this specimen, matrix crack formation has been suppressed, and clustering of the non-aligned fiber breaks is observed. The extensive matrix damage around the fiber breaks occurred when the applied stress on the specimen was removed. However, the absence of this type of deformation in the non-touching 2-D array suggests that the matrix deformation is higher surrounding the fiber breaks in the touching fiber

specimen. In addition, this matrix damage along with the location of each fiber break has been observed by OCT (Figure 6). Capitalizing on OCT's unique ability to see changes in matrix stresses, the area immediately surrounding the fibers has a different intensity than the bulk resin (Figure 7). This intensity change reflects the residual curing stresses that occur due to the close proximity of the fibers. This change in intensity is not observed in single fiber fragmentation specimens, and these stresses may influence the observed failure behavior.

In previous research on single-fiber specimens, we have noted that the matrix is non-linear viscoelastic. However, reconciling this effect with the occurrence of brittle fracture in composite specimens has been problematic. A 2-D multi-fiber array specimen was taken in several steps to a strain level that induces fiber fracture. During a period of 5 min, numerous non-aligned fiber breaks occur in the observation region, reflecting the role that the matrix has on the stress redistribution process in adjacent fibers after fiber fracture (see video at website: <http://polymers.msel.nist.gov/researcharea/multiphase/project-detail.cfm?PID=56>). At the end of this period the specimen failed in a brittle manner away from the observation region. This video indicates that the nucleation of the critical flaw that induces brittle composite failure may be time dependent and controlled by the viscoelastic matrix and the mode of interphase failure that accompanies fiber fracture.

Conclusions

Consistent with epoxy compatible industrial coatings, the 11-AUTCS coating has shown a propensity to form matrix cracks in addition to fiber-matrix debonding during fiber fracture. Initial investigations revealed the presence of 45° shear deformation bands emanating from the crack tips when the specimens are under tensile load. The shape of the matrix cracks surrounding each fiber break is similar to asymmetrical penny shaped cracks. It is known that penny shaped cracks in a material subjected to uniaxial tensile loads generate 45° deformation shear bands that form relative to the tensile axis at the crack-tip. The deformation bands emanating from the crack tips may be related to this phenomenon. The location of the penny shaped flaws within the composite is controlled by the spatial population of flaws in the embedded fiber and the stress transfer efficiency at the fiber-matrix interface. The influence of these shear bands on the non-aligned fiber break patterns shown in this figure is not known. It is believed at this point that these bands may be an important key to understanding the role that the viscoelastic matrix plays in nucleating critical flaws in fibrous composites. Finally, OCT has been used to model the failure region around the breaks and the residual stresses surrounding the fibers upon processing.

Bibliography

1. Kelly, A and Tyson, W, *J. Mech. Phys. Solids* **13**, 329-350 (1965).
2. Cox, H.L., *British Journal of Applied Physics*, **3**, 72-79 (1952).
3. Holmes, G.A., Peterson, R.C., Hunston, D.L. and McDonough, W.G., *21st Annual Meeting of the Adhesion Society*, 175-178 (1998).
4. McDonough, W., Holmes, G. and Peterson, R., *Proceedings of the 13th Annual Technical Conference on Composite Materials*, American Society for Composites, 1688-1695 (1998).
5. Drzal, L.T. and Herrera-Franco, P.J., *Engineered Materials Handbook: Adhesives and Sealants*, **3** (ASM International), 391-405 (1990).
6. Holmes, G.A., Peterson, R.C., Hunston, D.L. and McDonough, W.G., *Polymer Composites*, **21**, 3, 450 (2000)
7. McDonough, W.G., Dunkers, J.P., Holmes, G.A., Feresenbet, E., Kim, Y.H. and Parnas, R.P., *Polymer Composites*, in press.
8. Sastry, A.M. and Phoenix, S.L., *J Mat Sci Lett*, **12**, 1596-1599 (1993).

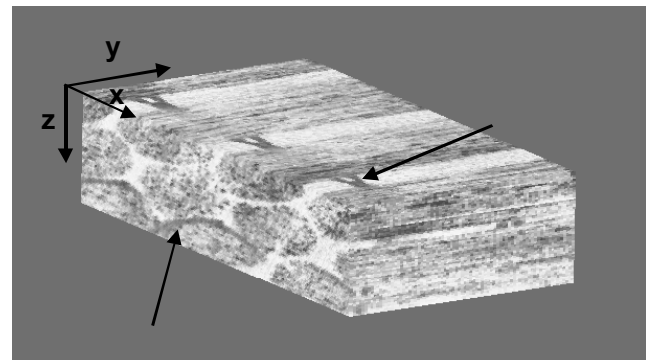


Figure 1: OCT volumetric reconstruction of an epoxy/unidirectional E-glass composite.

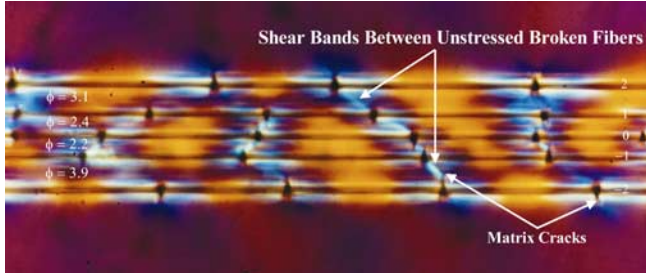


Figure 2: Image of the failure zone where the fibers are not touching.

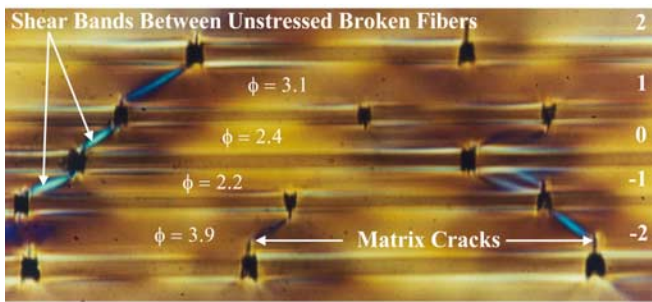


Figure 3: Image of the failure zone taken 24 h after the image in Figure 3.

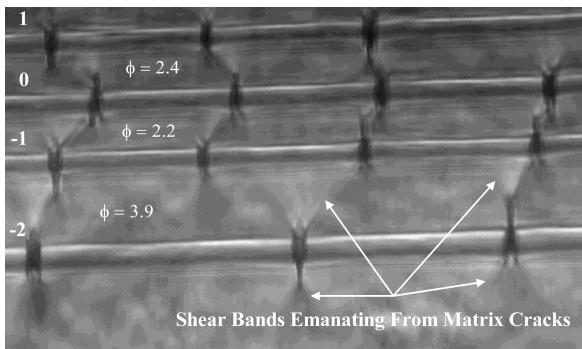


Figure 4: Image taken from the automated fragmentation testing machine showing the connections between the shear bands and the cracks in the fibers.

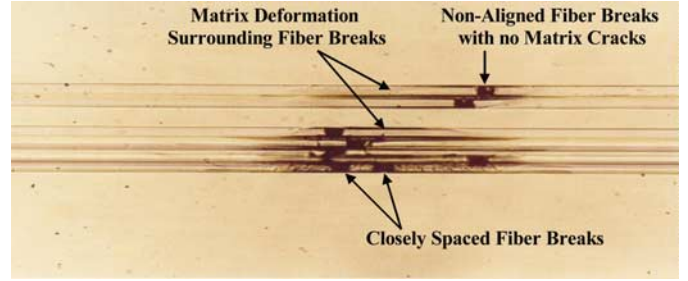


Figure 5: Image from a specimen where the fibers touched each other. Note the extensive damage in the matrix along the fibers.

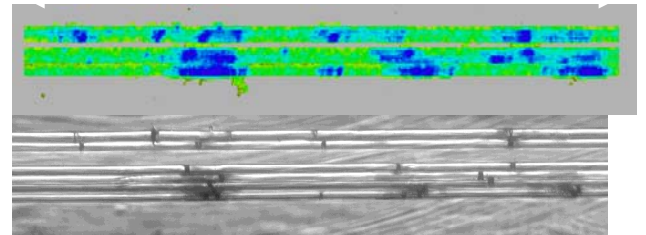


Figure 6: Comparison of the OCT image (top) with an image from the fragmentation apparatus showing OCT's ability to image damage along the interface between the fiber and matrix.

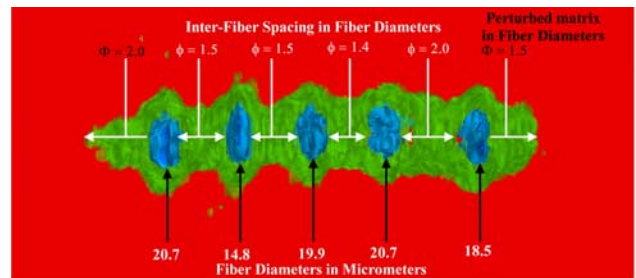


Figure 7: OCT image of a 2-D array of fibers looking end-on. Note the deformation in the matrix caused by residual stresses. . The standard uncertainty of the measurement of the fiber diameter was $0.3 \mu\text{m}$.

Key words: interface, failure behavior, optical coherence tomography